

Geophysical and hydrological investigations at the west bank of Nile River (Luxor, Egypt)

M. Elwaseif · A. Ismail · M. Abdalla ·
M. Abdel-Rahman · M. A. Hafez

Received: 29 July 2009 / Accepted: 9 January 2012 / Published online: 26 January 2012
© Springer-Verlag 2012

Abstract Luxor, the modern Egyptian city that occupies the site of ancient Thebes, is famed for its magnificent ancient monuments. Since 1967, the Aswan high dam has prevented the annual flooding of the Nile River, resulting in excessive salt accumulation on the Nile floodplains and on exposed monument surfaces. In addition, the expansion of agricultural land within the Luxor study area has resulted in increased salinity and groundwater level. These conditions accelerate the degradation of buried and exposed monuments that were fairly well preserved in the past. To mitigate this problem, it is necessary to first understand the near-surface setting and the groundwater conditions of the Luxor area. A geophysical investigation was carried out using resistivity and electromagnetic surveys. In addition, a chemical analysis was conducted of some surface water samples collected from canals and the sacred lake of Memnon Temple. Based on the results of the geophysical surveys and the chemical analysis of the water samples, the shallow subsurface was characterized into four geoelectrical units. Groundwater flow directions were determined to be from the central area to the west, causing

a rise in the groundwater levels and groundwater salinity in the area of monuments.

Keywords Joint inversion of VES and TEM · Hydrogeology · Salinization · Luxor (Egypt) · Nile River

Introduction

Luxor, Egypt, occupies the site ancient Thebes, which was known for its buildings and many large gates. The west bank of Luxor (Fig. 1) contains more than 30 known limestone temples, most of them built by the rulers of the New Kingdom (1549–1069 BC). Both buried and exposed archeological features are affected by the high level of saline groundwater at the west bank of Luxor area since the construction of Aswan high dam and the resultant expansion of agricultural lands around the temples' area. Saline groundwater is transported into the monuments' foundations through underlying soil by means of capillary rise. When those saline waters evaporate, residual salts accumulate on the surface and within the pore spaces of the foundations. The pressure developed during the crystallization and hydration of the residual salts exfoliates the outer layers of the foundations' stone, increasing their susceptibility to erosion by wind and other physical processes (Rodriguez-Navarro and Doehne 1999). Figure 2 shows an example of the monuments' degradation at Habu Temple in the west bank of Luxor.

Geophysical methods have been widely applied to groundwater exploration (e.g., Asfahani 2007; Ismail 2003; Albouy et al. 2001). Asfahani (2007) employed vertical electrical sounding (VES) at the Khanasser Valley (Syria) and successfully identified the nature and geometry of a deep aquifer. Ismail (2003) conducted a study to mitigate

M. Elwaseif (✉) · A. Ismail · M. Abdalla · M. A. Hafez
National Research Institute of Astronomy and Geophysics
(NRIAG), Helwan, Cairo, Egypt
e-mail: Mehrez@andromeda.rutgers.edu

M. Elwaseif
Department of Earth and Environmental Sciences,
Rutgers, The State University, Newark, NJ, USA

A. Ismail
Illinois State Geological Survey, 615 East Peabody Drive,
Champaign, IL, USA

M. Abdel-Rahman
Ain Shams University, Abbassia, Cairo, Egypt

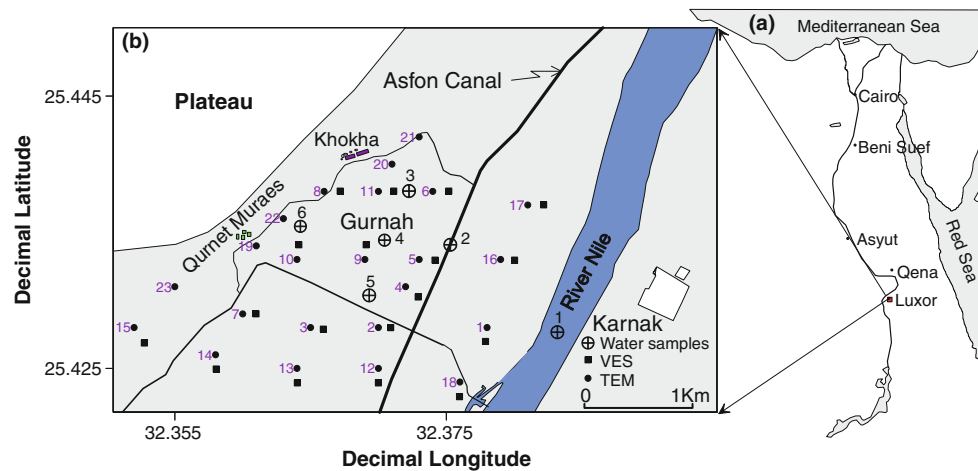


Fig. 1 Location map of **a** Egypt, and **b** Luxor study area including the locations of collected water samples, VES and TEM data



Fig. 2 Effects of shallow saline groundwater on the Habu temple (note the severe cracks and salt accumulations)

the degradation of monuments on the east bank of Luxor, employing VES and seismic surveys to characterize the hydrostratigraphy of the shallow subsurface. Albouy et al. (2001) examined the merits of using VES and transient electromagnetic (TEM) methods for coastal groundwater exploration, north of Biarritz and at two selected sites at the flanks of le Piton de la Fournaise, France. Those scientists showed that the joint inversion of VES and TEM data are an efficient tool to resolve the ambiguity of each measurement method alone, especially in the absence of supportive geological information, such as well-log data.

The TEM method is an electromagnetic induction technique by which the response of the earth to an electromagnetic impulse is measured in the time domain. The VES method uses direct current to measure the resistance of the subsurface using grounded steel electrodes. Although electrical resistivity and electromagnetic techniques measure the same physical property, soil resistivity, the techniques are sensitive to different characteristics (Gomez-Trevino and Edwards 1983; Raiche et al. 1985). Well-resolved electrical resistivity data obtained using the VES method are the product of layer resistivity and layer thickness (Fitterman et al. 1988). Such data do not provide

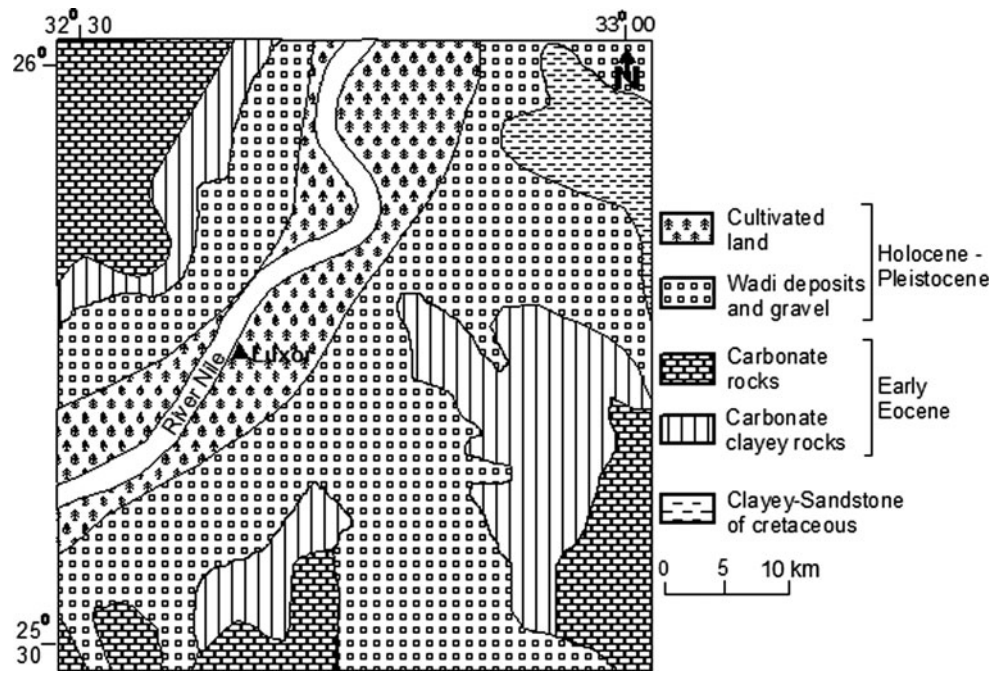
good independent estimates of layer resistivity and layer thickness. In contrast, electromagnetic methods are good for establishing the thicknesses of layers but not their resistivity values (Fitterman et al. 1988). The combined inversion of TEM and VES data constrains the resistivity-depth geophysical model, and reduces ambiguities in the interpretation of the measurements (Sasaki 1989; Sandberg 1993; Albouy et al. 2001).

In this study, a large-scale geophysical survey was conducted and chemical analysis performed of surface water samples at the west bank of the Nile River (west Luxor area) to characterize the near subsurface hydrogeologic setting and to identify the sources responsible for increasing the salinity of groundwater. The geophysical survey is in the form of integrated TEM and VES measurements. The groundwater analysis included chemical analysis of six surface samples collected from the areas adjacent to the degraded monuments. The results of this study will be critical to developing conservation plans for the existing archeological structures.

Study area

The study area, located on the alluvial plains of the Nile Valley and surrounded by elevated structural plateaus capped by Eocene limestone, is underlain by Paleocene shale (Fig. 3). The alluvial plains generally exhibit flat surfaces that gently slope northward. The average ground surface elevation is about 75.5 m above the mean sea level, but rises to about 79 m at the fringes of the Nile Valley. These alluvial plains can be differentiated into (1) a densely cultivated younger plain occupying the central part of the Nile Valley and covered by Holocene silt and clay, and (2) an older reclaimed plain covered by Pleistocene sand and gravel (El Hosary 1994; Research Institute of Groundwater 1997).

Fig. 3 Geologic map of Luxor area (El Hosary 1994)



The near-surface Pliocene–Holocene sediments in the central part of the Nile Valley rest uncomformably on a succession of Late Cretaceous–Early Eocene marine sediments (Fig. 4). The Pliocene–Holocene sediments have been subdivided into different lithological units, each of which was deposited by an identified ancestral-modern river system (Ismail 2003), including the Eonile, Paleonile, Protonile (Q1), Prenile (Q2), and Neonile (Q3).

Two main aquifer systems are distinguished within the Pliocene–Pleistocene in the Luxor study area: the shallow Quaternary aquifer and the underlying Pliocene–Pleistocene aquifer. The Quaternary aquifer is composed mainly of graded sand and gravel and locally the thickness ranges from 5 to 95 m and salinity is about 2.6 mg/L. The underlying Pliocene–Pleistocene aquifer, composed of sand and clay, is the secondary aquifer in the study area and has an average salinity value of 700 mg/L (Ismail 2003).

Geophysical data acquisition and processing

Eighteen VESs were acquired using the Syscal R2 instrument (Fig. 1). The Schlumberger electrode configuration was employed, and the maximum current electrode spacing (AB/2) varied from 300 to 400 m. The VESs were spaced at 0.5 to 1-km intervals. The measurements were taken in the east–west direction, perpendicular to the Nile Valley. The measured apparent resistivities from each VES were plotted simultaneously against AB/2 values on log–log paper in the field for quality control of the data.

A suite of 23 TEM soundings were measured using the SEROTEM system close to the locations of the resistivity measurements. A simple coincident loop configuration was employed; in this configuration, the same loop transmits and receives signals. The loop side length was 50 m. During data acquisition, measurements were repeated several times to ensure a high signal-to-noise ratio.

Due to the lack of boreholes at the study site and in order to roughly control the VES interpretation, the present study used the litho-resistivity model of Ismail (2003), based on two boreholes located about 200 m away from the acquired VESs at the east bank of Luxor. In that model, four litho-resistivity units were characterized: (1) an upper unit of dry silty clay with relatively high resistivity (~20 ohm-m), (2) a lower unit with significantly low resistivity (~4 ohm-m) assigned to the moist silty clay, (3) a thick unit (>20 ohm-m) with high resistivity assigned to the main Quaternary aquifer layer, and (4) a low-resistivity layer (<4 ohm-m) assigned to a secondary aquifer layer (Fig. 5a, b).

The resistivity data were first inverted in terms of one-dimensional (1-D) resistivity-depth models using software described by Zohdy (1989) and Meju (1991). The output models were used as initial models for inverting the nearby TEM data using TEMIXXL (1996) software. The resultant TEMIXXL models were used again as initial models for inverting the resistivity data in RESIST (Vander 1988) software. The misfit errors between the measured and calculated models for the whole data set range from 2.8 to 7.3% (Fig. 5c, d). This iterative method was continued until reliable resistivity-depth models were obtained that

Fig. 4 Composite stratigraphic column at Luxor area (El Hosary 1994)

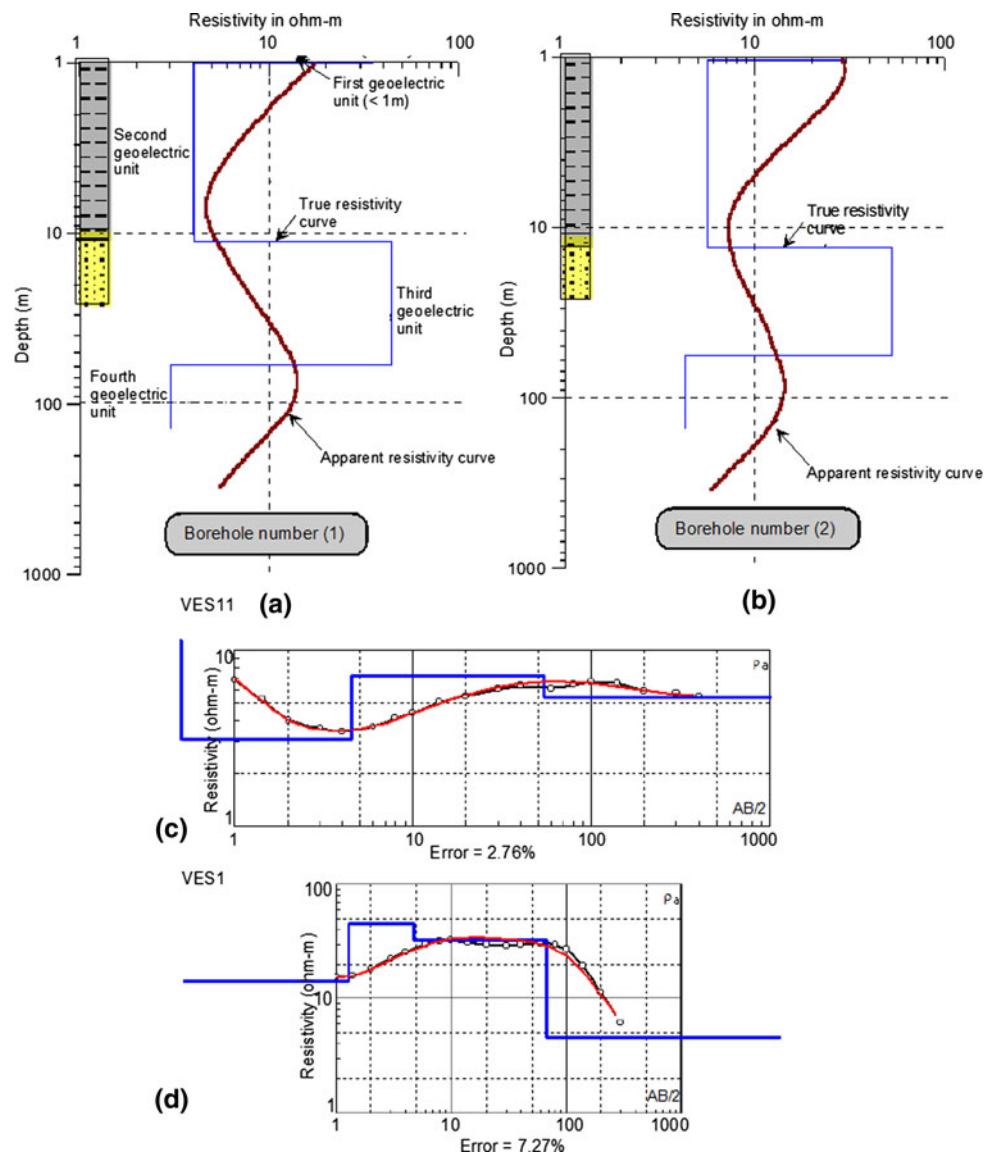
Age		R. Stage	Formation	Lithology	Description	
Quaternary	Holocene	Neonile (Q3)	Arkin		Gravel and Sand	
					Silty clay of cultivated land	
	Pleistocene	Middle - Late	Prenile (Q2)	Abbassia		Conglomerate
				Dandara		Sand silt and clay
				Abbassia		Conglomerate
				Qena		Massive cross-bedded sand with clay lenses
		Early	Proto. Prenile (Q1/Q2)	Issawia		Tuffa, red breccia and sand
				Amant		Clay, sand and conglomerate
	Tertiary	Pliocene	Paleo-Nile	kdfu		Cobbles and gravels in red clay matrix
				Madmud		Red brown clay, sand, silt and marl
Eocene		Early	(Te)	M. Seq.		Clay and sand
				Thebes		Chalky limestone bed with chert bands
Paleocene		(TP)	Esna		Marls and shales	
			Tarwan		Chalks	
Cretaceous		Late	Kda	Dakhla		Chalks and marls
				Duwi		Marls, shales, and phosphates
				Nubian		Sandstone with shale

seemed to be consistent with the subsurface geologic setting. The final models were interpolated to generate 2-D resistivity cross sections, parallel and perpendicular to the Nile River.

VES and TEM results

Based on the joint inversion of resistivity and electromagnetic data, two geoelectrical resistivity cross sections

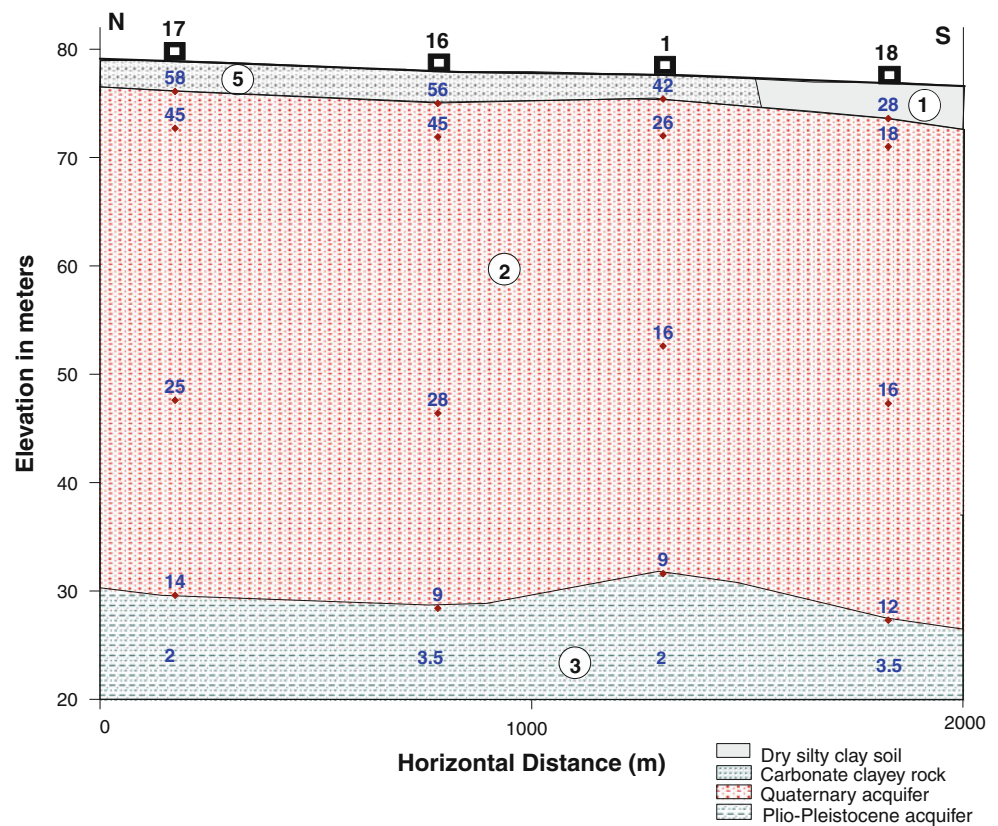
Fig. 5 Calibration of the measured apparent resistivity with the corresponding lithologic units at two boreholes (a, b), c and d are the processing results of two VESs (after Ismail 2003)



were generated, one parallel to the Nile River and the other perpendicular to the Nile (Figs. 6, 7). The geoelectrical resistivity cross sections exhibit four geoelectrical units. No significant lateral resistivity variation was found within individual units:

1. The first (upper) geoelectrical unit consists of (1) a relatively dry silty clay agricultural soil less than 4 m thick with resistivity values ranging from 5 to 28 ohm-m, and (2) dry silty clay and gravel soil, having a resistivity value of 50 ohm-m and a thickness of 2 m.
2. The second geoelectrical unit consists of sand, silt, and gravel of the main Quaternary aquifer. The average resistivity value is 20 ohm-m, and thickness is about 48 m. The thickness of the aquifer layer decreases significantly toward the west plateau.
3. The third geoelectrical unit is characterized by low-resistivity value (<5 ohm-m) and thickness ranging from about 4 m near the Nile River to about 48 m near the western plateau. This unit represents the secondary aquifer in the study area (Pliocene–Pleistocene aquifer). The significant resistivity contrast between the Quaternary aquifer and the underlying Pliocene–Pleistocene aquifer is attributed to the higher salinity (700 vs. 2.6 mg/L) and clay content of the sediments within the Pliocene–Pleistocene aquifer (Ismail 2003).
4. The fourth geoelectrical unit is characterized by a resistivity value of about 10 ohm-m. This unit appears only at the base of the plateau area at a depth of 2–5 m. This unit represents the Paleocene shale layer. Its low resistivity is due to the lateral seepage of groundwater

Fig. 6 Geoelectrical cross section extending parallel to the River Nile



from the adjacent Pliocene–Pleistocene aquifer. A normal fault separates the third and fourth units, and this fault was traced on the resistivity section of Fig. 11. The location and orientation of this fault seem to be consistent with the major fault forming the Nile Valley in this area (El Hosary 1994).

The inverted resistivity, or “true” resistivity, of each of the specified geoelectric units was mapped to better demonstrate the lateral resistivity variation with depth and its possible impact on the degradation of the area’s monuments.

Resistivity distribution at 1 m depth

The first unit represents the dry silty clay topsoil. The resistivity values of this unit vary from 5 to 75 ohm-m (Fig. 8). Although surface conditions, such as farming and urbanization, affect resistivity distribution, the values still provide a good indication of the moisture and/or salinity distribution within the topsoil, which is in direct contact with the archeological features. The high-resistivity values of 25–75 ohm-m are observed near the urban areas (parallel to the Nile River) and near the limestone plateau. The low-resistivity values of less than 24 ohm-m are found for the central cultivated areas in the study site. These low values are a direct result of increased-moisture content due

to irrigation and increased salinity caused by excessive evaporation and use of fertilizers.

Resistivity distribution at a depth of 4 m

This unit has resistivity values range from 3 to 29 ohm-m and is characterized by three main resistivity zones (A, B and C), which correspond to the second, third, and fourth geoelectrical units, respectively (Fig. 9). Resistivity values range from 10 to 29 ohm-m for Zone A, which represents the saturated sand and silt sediments of the Quaternary aquifer. The water within this aquifer seems to be fresh and originating from the Nile and irrigation canals (e.g., Asfon canal) in the study area. The resistivity value is low (5 ohm-m) for Zone B, which represents the Pliocene–Pleistocene aquifer in the study area. Zone C, representing the Paleocene shale, has resistivity values ranging from 8 to 16 ohm-m, probably because of its high-moisture content and/or salt.

Resistivity distribution at 48 m depth

This unit has low-resistivity values ranging from 1 to 7.5 ohm-m. Although the range is narrow, Zones B and C are obvious, as shown in Fig. 10. Zone B resistivity values range between 2.5 and 7.5 ohm-m. This zone is probably

Fig. 7 Geoelectrical cross section extending perpendicular to the River Nile

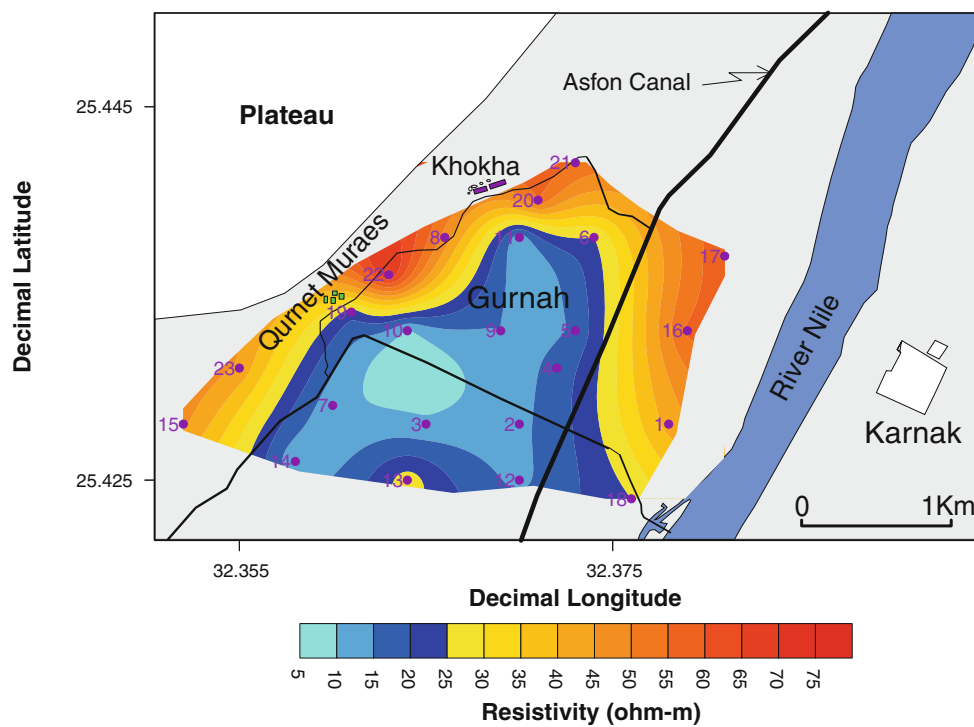
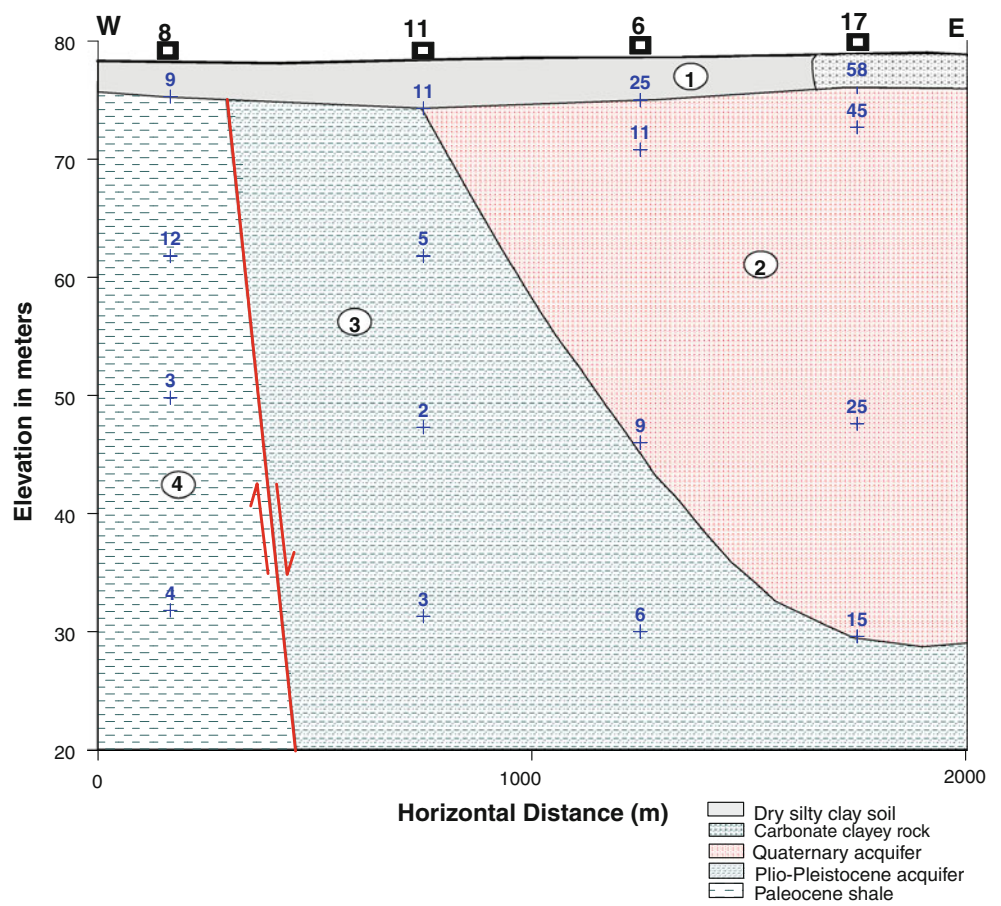


Fig. 8 Spatial resistivity distributions at 1 m depth

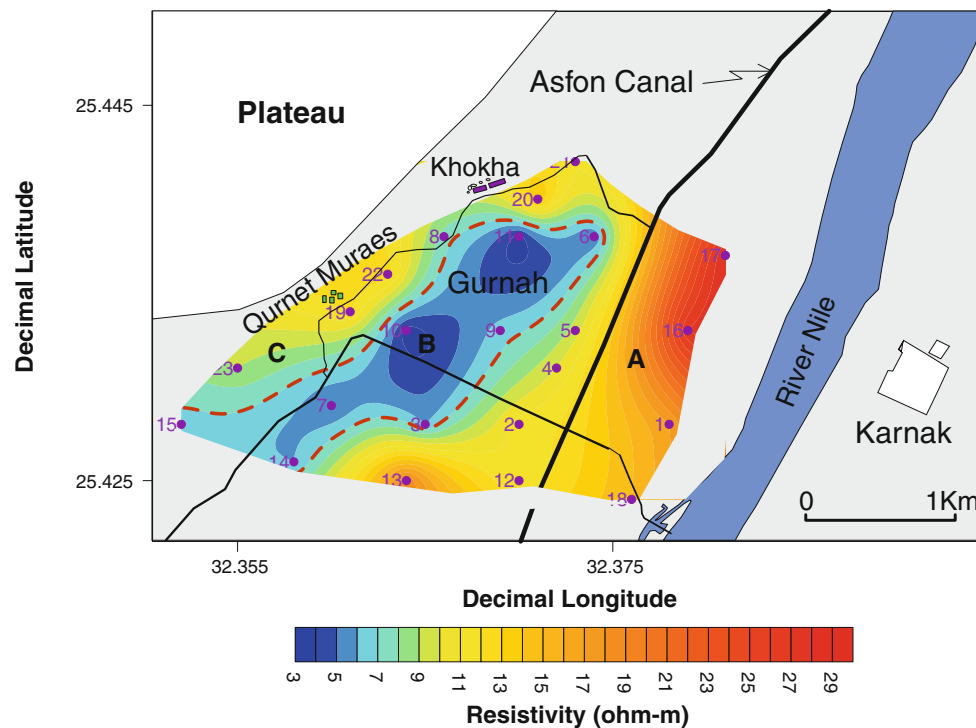


Fig. 9 Spatial resistivity distributions at 4 m depth

an extension of the Pliocene–Pleistocene aquifer that consists of sand with clayey sediments. Zone C, which corresponds to the moist Paleocene shale layer, exhibits a very low-resistivity value of 2 ohm-m.

To better visualize the surface and subsurface at the study site, we constructed a composite model that shows the spatial resistivity distribution of subsurface geoelectrical units, the surface location of temples, cultivated areas, and the Nile River. As shown in Fig. 11, the Nile River does not contribute to the groundwater recharge in the study area, since the resistivity values of different strata increase toward the east (i.e., toward the Nile), which is consistent with the conclusion of Ismail (2003). The groundwater flow seems to flow from west to east, and, in the surface layer, from the cultivated areas outward.

Chemical analysis of the water samples

Results of the chemical analysis of water samples can be integrated with the geophysical interpretation to yield valuable information on the causes of increasing salinity and groundwater level at Luxor study area. Six surface water samples were collected from the study area from the Nile River, the canals, and the sacred lake of Memnon Temple. The results of the chemical analyses are presented

in Table 1. The sources of different ions in the examined water could be grouped as follow.

Cultivated lands

Sodium (Na^+), an essential constituent used in fertilizers (e.g., Phillips et al. 2001), was 195 ppm in water sampled at Memnon Temple compared with 36 ppm from the River Nile. The high-sodium concentration observed at the temple is evidence that the water inside the monument migrated from the nearby cultivated lands.

Potassium (K^+) is an essential plant nutrient (e.g., Mengel and Kirkby 1980). Potassium is highest (3.5 ppm) in the water sample taken from Memnon Temple, again supporting the interpretation that this water migrated from the surrounding cultivated areas.

Sulfate (SO_4^{2-}) is derived from gypsum, acid rains, and fertilizers (Garg 1978). The highest concentration (96 ppm) of sulfate is observed at Memnon Temple, indicating that its water probably comes from nearby cultivated areas.

Chloride (Cl^-) is mostly presented either as salt crystals or in solution (Na^+ and Cl^- ions) (Hem 1970). The concentration of chloride ranges from 21 ppm at the eastern side of the study area to 190 ppm at Memnon Temple. The high concentration of chloride at the temple is related to the successive accumulations of water inside the temple that probably migrated from cultivated areas.

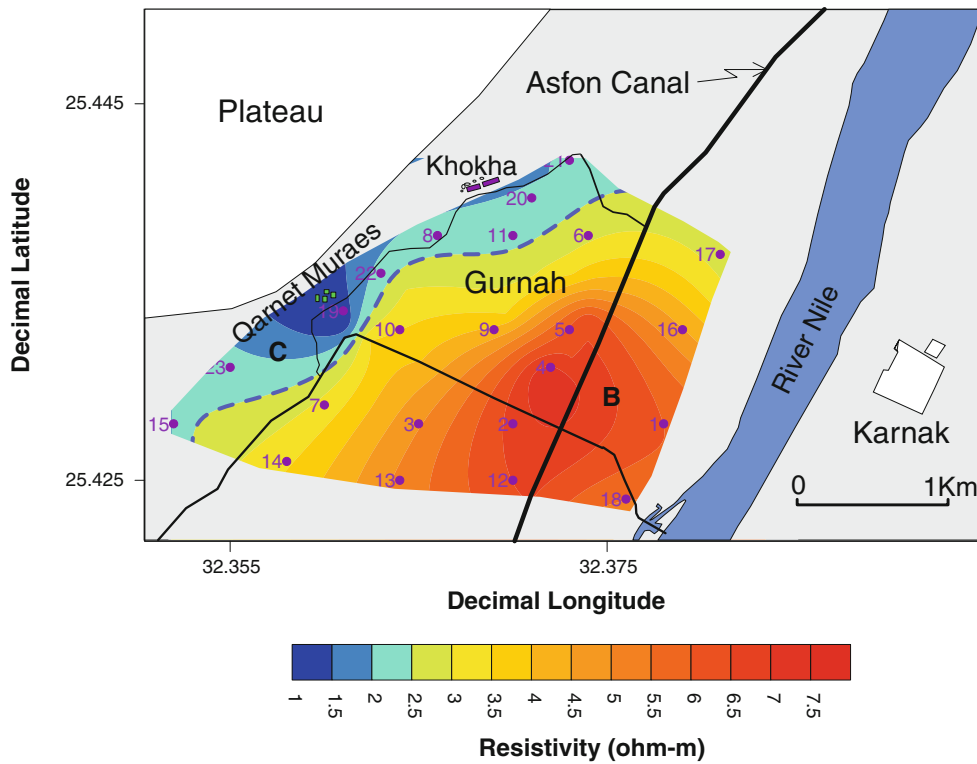


Fig. 10 Spatial resistivity distributions at 48 m depth

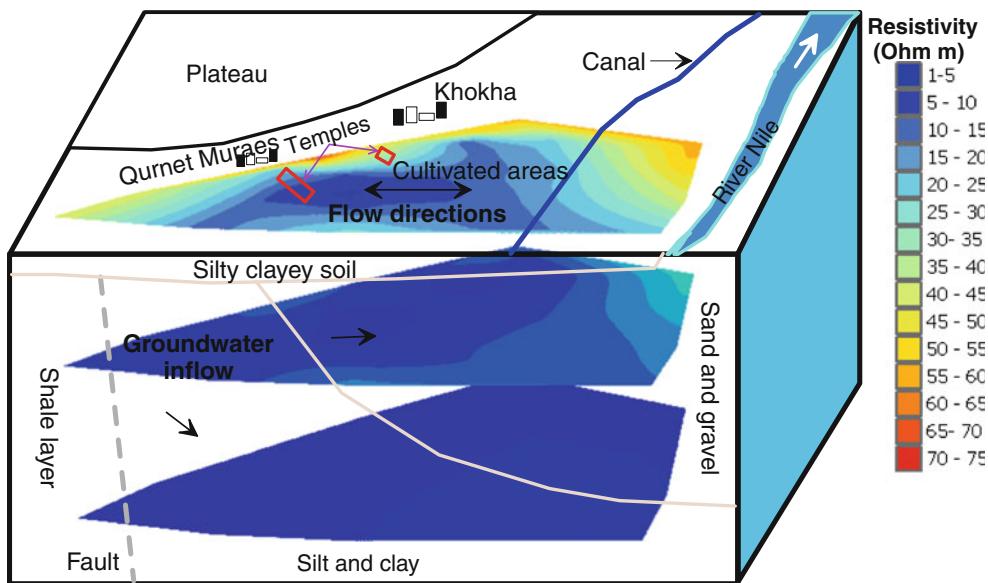


Fig. 11 Composite model of Luxor study area

Weathering of monuments/temples

Calcium (Ca^{2+}) and magnesium (Mg^{+2}) are the principal minerals forming carbonate rocks such as limestone ($CaCO_3$) and dolomite ($CaMg [CO_3]_2$). The highest calcium

(22 ppm) and magnesium concentrations (18 ppm) were observed at Memnon Temple, probably due to the dissolution of carbonate rocks forming its stone foundations.

Bicarbonates (HCO_3^{-1}) are formed when carbon dioxide is dissolved or derived from limestone (e.g., Rogers et al.

Table 1 Results of geochemical analysis of water samples (Fig. 5 shows the location of these samples)

Sample no.	pH	TDS	Anions (ppm)				Cations (ppm)				EC
			CO ₃ ⁻²	HCO ₃ ⁻¹	Cl ⁻¹	SO ₄ ⁻²	Na ⁺¹	K ⁺¹	Ca ⁺²	Mg ⁺²	
1	8.3	217.6		122	28	28	36	1.17	16.5	12	340
2	8.2	211.2		134	22	23	41	1.17	14	9.5	330
3	8.2	211.2		122	25	28	38	1.17	12	12	330
4	8.2	217.6		134	24.5	24	38	1.6	14	12	340
5	8.3	204.8		134	21	19	41	1.17	10	11	320
Temple	8.3	716.8	30	354	190	96	195	3.5	22	18	1,120

1985). The bicarbonate concentration of water sampled from the Nile River is 122 ppm; from the irrigation channels, 134 ppm and at Memnon Temple, 354 ppm. The high concentration of bicarbonate at Memnon Temple is because of the dissolution of the limestone of its stone foundations.

Natural sources

The pH value of water is a measure of the concentration of hydrogen ions (H⁺). The pH values of the water samples from the study area vary between 8.2 and 8.3, indicating alkalinity and the dissolution of calcium and magnesium ions in the water samples (e.g., Psenner 1988). Electrical conductivity of surface waters increases from east (320 micro S/cm) to west at Memnon Temple (1,120 micro S/cm). Water with high-electrical conductivity contains sodium and magnesium cations as well as calcium, chloride, and bicarbonate anions (e.g., Freund et al. 1993). As expected, total dissolved solids (TDS) was highest (716.8 mg/L) in the water sample collected from the sacred lake of Memnon Temple and lowest (204.8 mg/L) in the water samples from canals in the eastern side of the study area. The high-TDS value from the Memnon Temple is due to the evaporation of the water in the temple's sacred lake.

Discussion and conclusions

The joint inversion of VES and TEM data and the results of chemical analyses of water samples were successfully integrated to generate a suite of geoelectric resistivity cross sections and subsurface maps. The main disadvantage of the employed techniques is the limited spatial subsurface coverage and the uncertainty when generating the 2-D cross sections. Obviously, 2-D/3-D techniques (e.g., resistivity and ground-penetrating radar) would produce more subsurface coverage and more accurate models. Those techniques, however, are probably not the best choice at

this site given the large survey area, time constraints, and most importantly, because the goal of this present study is not the detailed hydrogeology of the field site. Furthermore, the methods employed in the present study are inexpensive, data acquisition is quick, and achievable penetration depth can be very deep (depending on AB/2 spacing and the loop size of the TEM survey).

Study results indicate that the shallow subsurface in the Luxor study area is divided into four distinct geologic/hydrologic units. Such characterization represents the foundation of any plan to lower the groundwater level and decrease the salinity of capillary soil moisture in the area of the Luxor monuments. Shallow groundwater flow paths were expected to have originated from the recently cultivated areas, west of Luxor and to flow toward the River Nile. The elevated groundwater in the area of the temples appears attributable to flood irrigation of recently reclaimed lands lying on the alluvial/flood plain transition. The progressive increase in salinity along the groundwater flow path is reflected in the recent deposition of precipitated salts observed at Habu Temple (Fig. 2). Based on our interpretation of the acquired data and the field observations, the salt accumulation on the foundations of the monuments appears to be ascribable to salt transport by capillary water from the relatively high-salinity groundwater or from connate water in the silty clay unit.

As a final comment on the study area, recommendations are to avoid cultivation of crops that require much water and to regulate the use of agricultural chemicals in the areas of thin silty clay soil. Further recommendations are to conduct high-resolution geophysical surveys (e.g. 3-D electrical resistivity) and detailed chemical analysis of the water proximal to the Luxor monuments. These suggestions might reduce the groundwater discharge at the temple areas and reduce its effects on the stone foundations.

Acknowledgments The authors thank three anonymous reviewers and the associate editor for their comments that helped improve the quality of this manuscript.

References

- Albouy Y, Andrieux P, Rakotondraso G, Ritz M, Descloitres M, Join J, Rasolomanana E (2001) Mapping coastal aquifers by joint inversion of DC and TEM soundings: three case histories. *Groundwater* 39:87–97
- Asfahani J (2007) Geoelectrical investigation for characterizing the hydrogeological conditions in semi-arid region in Khanasser valley, Syria. *J Arid Environ* 68:31–52
- El Hosary M (1994) Hydrogeological and hydrochemical studies on Luxor area, southern Egypt. MSc Thesis, Ain Shams University, Cairo, Egypt
- Fitterman D, Meekes J, Ritsema I (1988) Equivalence behaviour of three electrical sounding methods as applied to hydrogeological problems. European Association of Exploration Geophysics, 50th Annual Meeting Technical Exhibition, The Hague, The Netherlands, p 21
- Freund F, Freund M, Batllo F (1993) Critical review of electrical conductivity measurements and charge distribution analysis of magnesium oxide. *J Geophys Res* 98(12):209–230
- Garg S (1978) Groundwater and tube wells. Oxford and IBH Publishing, Oxford, p 333
- Gomez-Trevino E, Edwards R (1983) Electromagnetic soundings in the sedimentary basin of southern Ontario: a case history. *Geophysics* 48:311–326
- Hem JD (1970) Study and interpretation of the chemical characteristics of natural water, 2nd edn. U.S. Geological Survey Water Supply Paper 1473
- Ismail A (2003) Geophysical, hydrological, and archaeological investigation in the east bank area of Luxor, southern Egypt, PhD thesis, Department of Geology and Geophysics, University of Missouri-Rolla, USA
- Meju M (1991) SLINy, V Ver. 1.1 A, A user-friendly Schlumberger resistivity forward and inverse modelling program. Schlumberger
- Mengel K, Kirkby EA (1980) Potassium in crop production. *Advan Agron* 33:59–110
- Phillips C, Tenlep S, Pennell K, Omed H, Chi P (2001) The effect of applying sodium fertilizer on the rate of digestion of perennial ryegrass and white clover incubated in rumen liquor, with implications for ruminal tympany in cattle. *Vet J* 161:63–70
- Psenner R (1988) Alkalinity generation in a soft-water lake: watershed and in-lake processes. *Limnol Oceanogr* 33:1463–1475
- Raiche A, Jupp D, Rutter H, Vozoff K (1985) The joint use of coincident loop transient electromagnetic and Schlumberger sounding to resolve layered structures. *Geophysics* 50:1618–1627
- Research Institute of Groundwater (1997) Hydrogeological map of Luxor area, Scale 1:100 000. Explanatory notes
- Rodriguez-Navarro C, Doehne E (1999) Salt weathering: influence of evaporation rate, super saturation and crystallization pattern. *Earth Surf Processes Landforms* 24:91–209
- Rogers JA, Muller LD, Davis CL, Chalupa W, Kronfeld DS, Karcher LF, Cummings KR (1985) Response of dairy cows to sodium bicarbonate and limestone in early lactation. *J Dairy Sci* 68(3): 646–660
- Sandberg S (1993) Examples of resolution improvement in geoelectrical soundings applied to groundwater investigations. *Geophys Prospect* 41:207–227
- Sasaki Y (1989) Two-dimensional joint inversion of magnetotelluric and dipole–dipole resistivity data. *Geophysics* 54:254–262
- TEMIXXL V4 (1996) Temix V.4 user's manual, Interprex, 468 p
- Vander V (1988) Resist, a computer program for the interpretation of resistivity sounding curves. An ITCD M. Sc. Research Project. ITCD, Delft, The Netherlands
- Zohdy A (1989) The use of Schlumberger and equatorial sounding in groundwater investigations near El-Paso, Texas. *Geophysics* 34:713–728